Improved Passivation of n-Type Poly-Si Based Passivating Contacts by the Application of Hydrogen-Rich Transparent Conductive Oxides

Leonard Tutsch, Frank Feldmann, Bart Macco, Martin Bivour, Erwin Kessels, and Martin Hermle

***Abstract*—In recent years, the incorporation of hydrogen into indium and zinc oxide based TCOs has been recognized as an effective technique to improve the charge carrier mobility and hereby to relax the transparency-conductivity tradeoff within the thin films. On the other hand, the process sequence of poly-Si/SiO_x based contacts typically requires an extra rehydrogenation step in order to improve the chemical interface passivation. This article addresses the combination of the two matters by studying the ability of both atomic layer deposited and sputter-deposited TCOs to serve as hydrogenation sources. Here, we demonstrate improved passivation of poly-Si(n)/SiO_x contacts subsequent to TCO coatings and postdeposition thermal treatments resulting in iV_{oc} values of up to 743 and 730 mV for planar and random pyramid textured surfaces, respectively. Thus, a high passivation quality could be obtained without the need of additional hydrogenation treatments. For the textured interface morphology, a substantial hydrogen flux toward the SiO_x region turned out to be essential. This could either be ensured by adjusting the hydrogen partial pressure during the TCO growth process or by the addition of a thin AlO_x layer, serving as a effusion barrier.**

***Index Terms*—Atomic layer deposition (ALD), dc magnetron sputtering, hydrogen, indium oxide, passivating contact, poly-Si, zinc oxide.**

I. Introduction

POLY-SI based passivating contacts [1] are considered as a very promising technology for the next generation of silicon solar cells [2], [3]. Applying the poly-Si/SiO_x contact scheme on the cell's rear side, a power conversion efficiency of 25.8% [4] in combination with a diffused emitter on the front side has been achieved. To further increase the implied voltage, here, the diffused emitter can be replaced by a second poly-Si/SiO_x layer stack, which polarity is opposing the rear side [5]–[7]. The resulting cell design, characterized by a high degree of symmetry between rear and front side processing, reminds of the hydrogenated amorphous Si (a-Si:H)-based heterojunction cell technology SHJ [8], which has already made it into industrial production.

For both contact technologies hydrogen plays an important role in the saturation of electronically active defect states, which would, otherwise, catalyze the charge carrier recombination in the vicinity of the interface to the Si absorber. In case of the poly-Si passivating contact a high-temperature anneal at T in the range of 700–1050 °C is typically applied for crystallization and dopant activation. During this treatment, most of the hydrogen is effusing from the contact structure. Hence, in order to improve the chemical interface passivation, hydrogen has to be incorporated again afterward. Here, atomic hydrogen, being more effective for this purpose as bound within a H_2 molecule [9] can be donated by a hydrogen plasma, e.g., via remote plasma hydrogen passivation (RPHP) [10]. Alternatively, it can be supplied by H-rich dielectrics like SiN_x [11]–[13] or AlOx [14], [15]. A subsequent thermal treatment is required to enable the hydrogen diffusion to the critical poly-Si/SiO_x/c-Si interface, unless the process temperature present during the deposition of these films is already sufficient to achieve this.

For relatively thick poly-Si layers the application of metal contacts that are fired through the hydrogen-containing dielectric is an option. However, very thin poly-Si films utilized on the front side are not resilient to such metal firing. Therefore, these sacrificial dielectrics have then to be stripped off again (compare, e.g., [16]) prior to metallization. For such thin poly-Si layers, a particularly appealing option would be to hydrogenate from a hydrogenated transparent conductive oxide (TCO). First, this would remove the need to strip off the dielectric layer used for hydrogenation, since the TCO can be contacted directly by the metal.

In addition, a TCO is needed on the front side anyhow since the thin poly-Si layers lack sufficient lateral conductivity for efficient charge carrier extraction.

The majority of the TCOs utilized for Si solar cells belong to the class of indium or zinc oxide. In recent years, several studies stressed the beneficial impact of adding hydrogen to the atmosphere during the growth of both In_2O_3 [17]–[21] and ZnO [22]–[24] based TCOs. In brief, the high electron mobility in hydrogen-containing TCOs (TCO:H) was related to the ability of hydrogen atoms, first, to act as singly charged donors [25],

Manuscript received December 19, 2019; revised February 13, 2020 and March 25, 2020; accepted April 23, 2020. Date of publication May 14, 2020; date of current version June 19, 2020. This work was supported by the German Federal Ministry for Economic Affairs and Energy (at Fraunhofer ISE) under Contracts 0324141B (Selektiv) and 03EE1031B (Pasodoble). *(Corresponding author: Leonard Tutsch.)*

Leonard Tutsch, Frank Feldmann, Martin Bivour, and Martin Hermle are with the Fraunhofer-Institut fur Solare Energiesysteme, Freiburg im 79110 Breisgau, Germany (e-mail: leonard.tutsch@ise.fraunhofer.de; frank.feldmann@ise.fraunhofer.de; martin.bivour@ise.fraunhofer.de; martin.hermle@ise.fraunhofer.de).

Bart Macco and Erwin Kessels are with the Department of Applied Physics, Eindhoven University of Technology, 5612 AZ Eindhoven, The Netherlands (e-mail: b.macco@tue.nl; w.m.m.kessels@tue.nl).

Color versions of one or more of the figures in this article are available online at https://ieeexplore.ieee.org.

Digital Object Identifier 10.1109/JPHOTOV.2020.2992348

second, to passivate acceptor-type cation vacancies within the TCO [26] and defects at the grain boundaries of polycrystalline films as well as, finally, their beneficial role in the crystallization process of solid phase crystallized TCOs [18].

The target of this article is now to study the ability of such TCO:H layers to serve as hydrogen source for defect passivation at the poly-Si/SiO_x/c-Si interface. In order to investigate this topic on a wide scope, several combinations of substrate type, poly-Si thickness, TCO materials, and postdeposition thermal treatment are tested experimentally. These include the comparison of the passivation properties on planar Si(100) and random pyramid-textured surfaces. The surface of textured wafers is often more demanding in terms of passivation [27], as the effective interface area is enhanced and typically several irregularities, such as tips, valleys, and ridges, are present.

In this article, we exclusively focused on n-type poly-Si electron contacts. As hydrogenation sources two types of TCOs are studied: Hydrogen-rich zinc oxide deposited by atomic layer deposition (ALD) and tin doped indium oxide sputter-deposited under varying hydrogen addition. Furthermore, the thermal budget required to obtain a high passivation level was quantified for two postdeposition thermal treatments at different temperatures: in air and in vacuum.

II. Experimental Approach

In order to quantify the charge carrier recombination, symmetric lifetime samples were prepared on n-type (100)-oriented float zone (FZ) and Czochralski (Cz) wafers of 200 μm thickness with a resistivity of 1 and 6 Ωcm, respectively. Selected samples were etched in KOH to receive a random pyramid surface texture and all wafers were cleaned according to the RCA cleaning procedure [29]. After the final HF dip, a thin interfacial oxide layer of $\sim$12 Å was grown thermally in a tube furnace at 600 °C for 10 min in N_2/O_2 atmosphere. Subsequently, phosphorus-doped a-Si:H layers were deposited on both sides using a Centrotherm cPLASMA 2000 PECVD tool [30]. The effective a-Si:H thickness was varied for different experiments. Afterward, the wafers received a 10 min anneal in a tube furnace in N_2 atmosphere at 900 °C, leading to a slight diffusion of phosphorus into the c-Si wafer and turning the a-Si:H film into poly-Si. Serving as a reference for the passivation level some of the samples were exposed to the process RPHP at 400 °C for 30 min. Other test structures were symmetrically coated on both sides with a TCO layer of an effective thickness of around 75 nm. This was partly done by dc magnetron sputtering, where a circular ITO target with a composition of In_2O_3/SnO_2: 90/10 wt.%, a diameter of 25.4 cm and a purity of 99.99% was sputtered under an applied power density of 0.4 W/cm² at a distance of 10 cm from the substrate. Oxygen and hydrogen were introduced along with argon during the sputtering process resulting in a total pressure of 0.27 Pa. Without the introduction of gases the background pressure, which presumably mostly consists of water vapor, was of the order of 10^{-4} Pa. Other samples were coated by Al-doped and intrinsic ZnO and/or AlO_x by means of thermal ALD in an Oxford instruments OpAL reactor using a substrate temperature of 200 °C [31]. AlO_x depositions were performed using trimethylaluminum and H_2O as precursors. ZnO films were prepared using diethylzinc and H_2O. Al-doping was introduced by alternating the ZnO cycles with AlO_x cycles in a supercycle fashion, where dimethylaluminumisopropoxide was used as Al-precursor [32], [33]. When applied in a solar cell or in contact resistivity test structures usually an HF dip is conducted before TCO deposition in order to remove the SiO_x layer, which has formed at the poly-Si surface during the high temperature anneal. However, we found that for passivation properties this ultrathin layer had no impact concerning sputter damage or rehydrogenation behavior, so in this article this HF dip was omitted in some cases [removed SiO_x interlayer: Fig. 2(b), ALD samples in Fig. 3, cleaned but with native oxide due to long storage time before ALD: Fig. 1(b)]. After TCO deposition, thermal treatments were performed both in air and in a vacuum. For air annealing, a conventional hotplate was used. During the vacuum annealing process the samples received a pulsed irradiation by a quartz heater. Here, the substrate temperature steadily increased with IR light exposure time. The passivation quality after relevant steps in the process sequence was quantified by photo conductance decay measurements using a Sinton WCT-120 lifetime tester [34] and expressed either in terms of the implied open circuit voltage iV_{oc} at one sun illumination or by the minority carrier lifetime τ_{eff} at a lower injection density of 10^{15} cm^{-3}. Here, an optical factor of 0.95 and 0.7 was applied for planar samples with and without TCO coating (affecting the antireflective properties), respectively, being increased to 1.05 and 0.8 for samples with random pyramid surface texture. The optical factors were determined via superimposing transient and generalized lifetime curves.

III. Results and Discussion

In the first test symmetrical planar lifetime samples with 40 nm thick poly-Si on both sides were annealed in ambient air with or without being sputter-coated in advance with ITO of varying hydrogen content. In Fig. 1(a), the passivation level between the respective processes is expressed in terms of implied open circuit voltage iV_{oc} at one sun illumination. Due to the comparatively defect-poor poly-Si/SiO_x/c-Si(100) interface characteristics and the supporting poly-Si(n)-induced field-effect, the iV_{oc} was already at a proper level of 715 mV after the poly-Si formation step and before any rehydrogenation process. For the rather thick poly-Si used in this experiment, the iV_{oc} was not degraded during the ITO deposition, in case no hydrogen was intentionally added to the process atmosphere. It is reported that sputtering can generate defects in the vicinity of the SiO_x passivation region [35]–[37]; however, the invasivity of the species coming from the plasma is strongly dependent on poly-Si thickness and interface morphology [35], [38]. Increasing the hydrogen partial pressure clearly increased the surface recombination velocity (reducing the iV_{oc} to 672 and 657 mV) after sputtering, which is a phenomenon we constantly observe but the mechanism behind is still under investigation. In [39], the intensity of the plasma radiation in the UV significantly increased when hydrogen was added to the argon working gas, likely affecting the surface passivation. However, in our case the

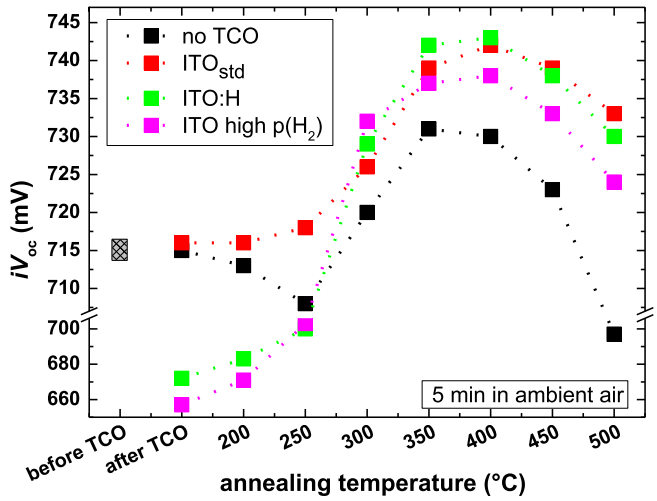

(a)

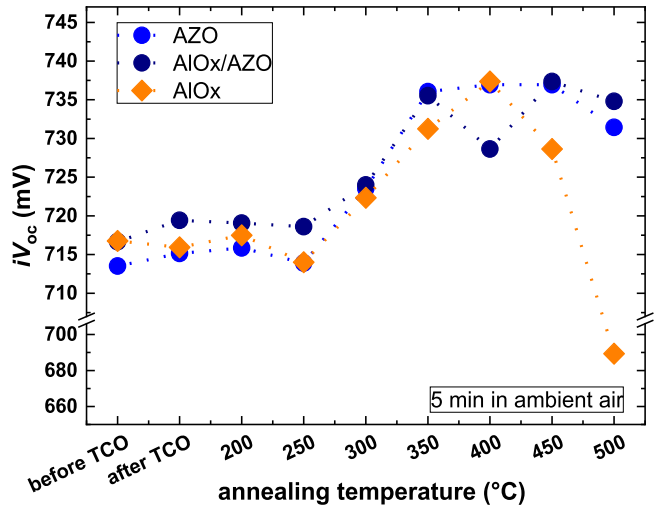

(b)

Fig. 1. Passivation level of planar FZ Si samples with 40 nm thick poly-Si (n) contacts. The lifetime samples were exposed to (a) ITO sputtering with different hydrogen concentration in the atmosphere or (b) ALD coated with AZO and/or AlO_x. Postdeposition thermal treatments were performed on a hotplate subsequently for 5 min at increasing temperatures.

induced defects were effectively curable and a high passivation quality could be achieved after conducting annealing steps at temperatures >300 °C for the low, moderate, and high hydrogen contents, peaking in an iV_{oc} of 742, 743, and 738 mV, respectively. Lying around 30 mV above the initial level this excellent passivation strongly indicates that not only the sputter-induced damage was annealed effectively but also hydrogen was released to support the saturation of defects at the SiO_x interface. This assumption is sustained by the drop in iV_{oc} for T $\geq$ 450 °C, which was related to the effusion of hydrogen out from the contact structure [40]. Note that the passivation of the reference sample without any TCO coating also improved up to 730 mV after exposure to 300 °C in air. This possibly originated from hydrogen entering from the ambient and/or from the relaxation of strain within the structure which can be present after the quite rapid cooling down after the poly-Si formation step. Here,

TABLE I
SUMMARY ERD AND RBS ANALYSIS OF ITO AND ITO:H

	H	In+Sn	O	Ar
	(atomic percentage, at.%)			
ITO$_{std}$	1.0	37.8	60.6	0.2
ITO:H	4.3	37.9	57.2	0.2

it can be mentioned that the lacking antireflective coating in this sample also affects the charge carrier injection at one sun illumination, which might have a slightly reducing impact on the iV_{oc} values. The reason for the effective boost in iV_{oc} in case of the nonintentionally hydrogenated ITO, denoted as ITO$_{std}$ in the following, can potentially be related to the comparatively high base pressure in the utilized sputter system. To compare the atomic composition of this ITO$_{std}$ layer and the films deposited under moderate H_2 addition (ITO:H) Rutherford backscattering spectrometry and elastic recoil detection (ERD) measurements were performed for as-deposited layers and summarized in Table I. The hydrogen content of about 1 at.% in the ITO$_{std}$ films might be sufficient to saturate residual dangling bonds in case of the planar c-Si(100) surface. Introducing hydrogen at a flow rate of 0.7 % of the total gas flow led to a hydrogen concentration of 4.3 at.% in the resulting ITO:H films. Interestingly, but being a side information in this context, the increase in hydrogen comes at the expense of oxygen atoms (60.6 to 57.2 at.%), whereas the relative metal (indium + tin) fraction stays constant at around 37.8 at.%.

Fig. 1(b) summarizes a similar study with AZO replacing ITO to check the ability of this hydrogen-rich ALD layer to work as a hydrogenation source. It was reported that a thin aluminum oxide capping can effectively prevent hydrogen to effuse out of the zinc oxide film [31] leading to an increased effective hydrogen diffusion flux toward the SiO_x interface. Hence, an AlO_x/AZO layer stack as well as a single AlO_x film were included. In both cases the AlO_x thickness amounted to 10 nm. As expected, no degradation in iV_{oc} occurred during the relatively soft ALD process, where no plasma was present. Again thermal treatments at T $>$ 300 °C improved the iV_{oc} to above 735 mV for all samples whereby the AlO_x capping was not beneficial here. Coating the poly-Si solely with the thin AlO_x film led to a reduction of passivation quality for T $>$ 400 °C, likely due to limited hydrogen reservoir in this layer. Nevertheless these experiments showed that it is relatively simple to achieve a good defect passivation in case of a planar Si(100) interface and thick poly-Si (n) contacts and a moderate amount of incorporated hydrogen is sufficient therefore. Noteworthy, the hydrogen content within the selected indium-and zinc oxide-based layers simultaneously enables suitable electro-optical properties of the respective films [32]. [41].

The next experiment then addressed the passivation properties on a random pyramid textured surface together with the impact of a reduced poly-Si thickness in order to investigate a contact structure more relevant for the cell's front side

As shown in Fig. 2(a), the initial iV_{oc} was now significantly lower ($\sim$660 mV), indicating the larger defect density at the

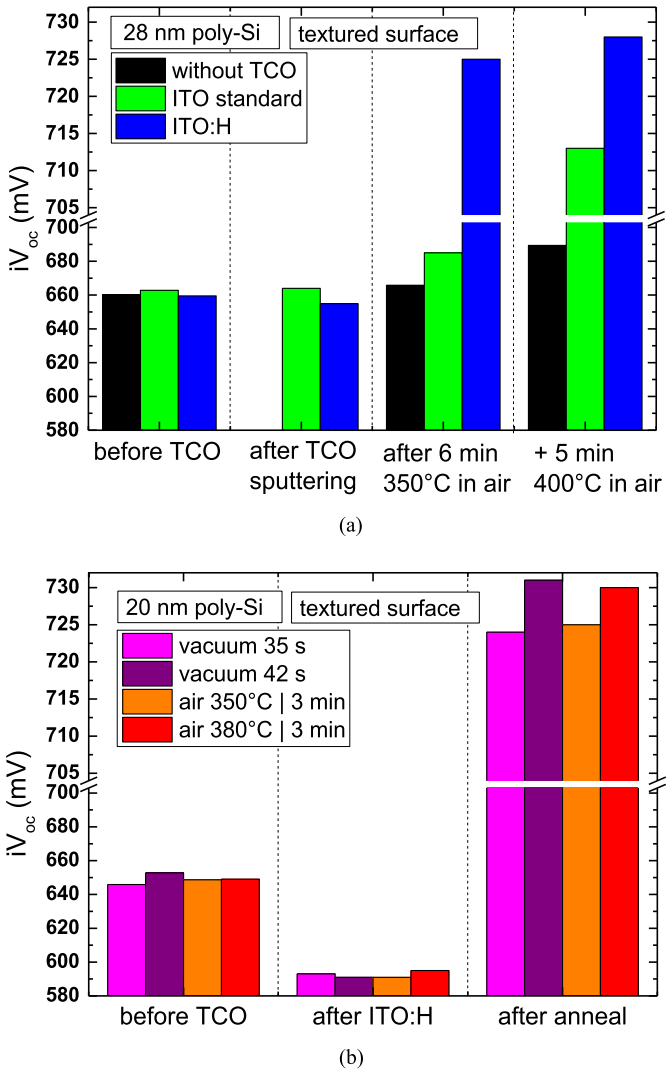

Fig. 2. Effect of surface texture and reduced poly-Si thickness. Symmetric textured samples containing (a) 28 and (b) 20 nm thick poly-Si layers were sputter-coated with ITO_{std} or ITO:H and received various annealing processes afterward.

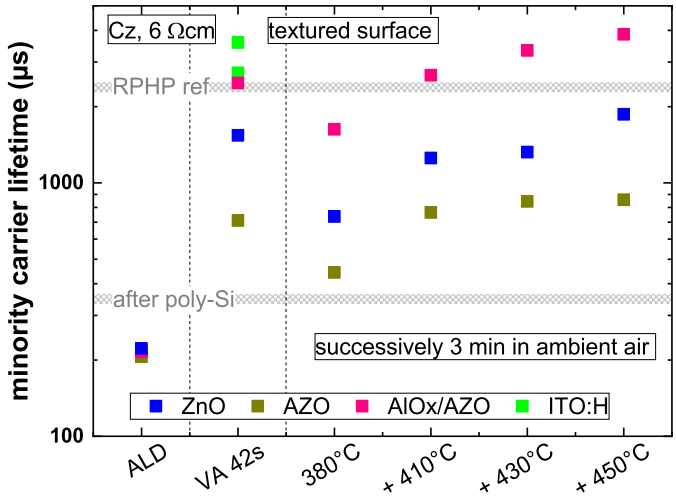

Fig. 3. Passivation level of textured CZ Si samples with 15 nm thick poly-Si (n) contacts. Various capping layers and annealing processes were applied on textured poly-Si(n)/SiO_x passivated Cz wafers.

textured interface. For the 28 nm thick poly-Si layer present here, the additional interface defects caused by the ITO sputtering with and without intentional hydrogen addition were hardly observable in the already low passivation quality.

Annealing the samples at 350 °C for 6 min in ambient air improved the passivation to 666, 685, and 725 mV in case of no capping layer, ITO_{std} and ITO:H, respectively. An additional 5 min exposure to 400 °C further increased the iV_{oc} values of these samples to 689, 713, and 728 mV. These results strongly indicated the relevance of a hydrogen containing capping layer for proper chemical passivation in case of the more challenging textured surface. A rather large thermal budget was required to achieve a moderate iV_{oc} for the hydrogen-poor ITO_{std} capping, whereas the hydrogen-rich ITO:H counterpart was already quite effective after the 350 °C anneal.

It has been reported that the electrical contact between the poly-Si and the TCO rapidly degrades during thermal treatments in ambient air at T $>$ 300 °C [35] Hence, as an alternative annealing process, we investigated dynamical infrared irradiation in vacuum, which was shown previously [38] to enable both low interface recombination and low contact resistivity. Fig. 2(b) depicts the iV_{oc} evolution during sputtering of ITO:H onto 20 nm thick poly-Si. For these thinner contacts, the additional defects generated during sputtering were reflected in a loss of around 50 mV to a level below 600 mV. The effectiveness of short (cumulated irradiation of 35 s) and longer (42 s) exposure to IR light in vacuum as well as of hot plate annealing in air at 350 °C and 380 °C for 3 min was quantified by iV_{oc} values of 723, 730, 725, and 730 mV, respectively. For the 42 s irradiation and the 380 °C hotplate anneal, the obtained passivation level was on par with the one achieved after an optimized RPHP step (∼730 mV, data not shown here).

Finally, to test the discussed processes on a layer structure simulating an optically well performing passivating front side contact, the poly-Si (n) layer thickness was further reduced to 15 nm. For this experiment, commercial Cz wafer were used and cut into 5 $\times$ 5 cm² substrates subsequent to the etching of random pyramids and the symmetrical application of SiO_x and poly-Si(n). The passivation level after various processes is shown in Fig. 3 and quantified this time by the minority carrier lifetime τ_{eff} at a fixed injection density of 10^{15} cm^{-3} in order to reduce the (slight) impact of the varying optical properties. Before any rehydrogenation treatment τ_{eff} was around 300 μs. After ALD deposition of either intrinsic (75 nm), or aluminum doped zinc oxide (75 nm), or AlO_x/AZO layer stacks (10/75 nm) the lifetime τ_{eff} was slightly reduced to 200 μs. Subsequently, the AZO, AlO_x/AZO, and ZnO coated samples were annealed in ambient air successively at 380, 410, 430, and 450 °C dwelling 3 min at each temperature point. Hereby, the lifetime in every sample gradually increased with temperature, peaking at 0.9, 3.9, and 1.9 ms, respectively, after the 450 °C step. Other samples, which had received the same ALD processes, were exposed to the 42 s irradiation step in vacuum, resulting in 0.7, 2.5, and 1.5 ms for AZO, AlO_x/AZO, and ZnO.

Receiving the same vacuum anneal, two substrates which were priorly sputter-coated with ITO:H showed τ_{eff} values of 2.7 and 3.6 ms. As a reference, samples exposed to the RPHP process showed a τ_{eff} of around 2.5 ms.

The results indicate that there is a certain temperature (>350 °C) required for hydrogen to become sufficiently mobile in order to migrate to the SiO_x interlayer and/or to overcome the activation energy for effectively supporting the chemical passivation at the poly-Si/SiO_x /c-Si interface region (compare, e.g., [15]). In particular, the binding of hydrogen to interface defects is attached importance when considering reported results on AlO_x/ZnO/SiO_x passivation [31], where already ample hydrogen was present at the SiO_x interface in the as-deposited state, but still a ∼400 °C step was required to activate the chemical passivation.

Moreover in case of the textured interface, the relevance of the AlO_x capping layer was now observable in the lifetime after both the air and the vacuum anneals. As studied in [31], the effusion of hydrogen from the ZnO to the ambient becomes significant at temperatures above 300 °C. Especially when bound to molecules hydrogen can pass quite easily through the ZnO grain boundaries. In case an AlO_x capping layer is omitted, the hydrogen flux toward the SiO_x is reduced. To what extent the hydrogen-rich AlO_x film itself has importance as a hydrogen source cannot be distinguished in this experiment.

The reason for the better performance of the intrinsic ZnO layers compared with the Al-doped counterpart for samples without AlO_x capping remains unclear. During the ALD supercycles the Al-doping is introduced in horizontal planes, which tend to disrupt the crystal growth. Since the ZnO grain boundaries are presumably an efficient transport path for hydrogen atoms, one hypothesis is that these horizontal planes by this means hamper the hydrogen transport. In contrast, an influence of the different work function of the TCOs on the interface passivation is considered improbable, due to the high doping level of the poly-Si layer in between.

IV. Summary and Outlook

In conclusion, it has been demonstrated that hydrogenation of n-type poly-Si contacts through hydrogenated TCOs can be highly effective. The passivation level of such contact structures could be improved significantly both by means of ALD and sputter-deposition of hydrogen-containing TCOs in conjunction with a postdeposition thermal treatment at temperatures above 300 °C. A differing behavior was observed between planar samples, where a first-rate interface passivation could be achieved even with hydrogen-poor ITO and AZO without capping layer, and their textured counterparts, which seemed to require a larger hydrogen content or an effusion barrier layer, respectively, together with a slightly elevated activation energy. Nevertheless, also in case of textured interface morphology a passivation quality on par with the RPHP reference could be achieved with both TCO types combined with air or vacuum annealing steps. As a feasible next step, ITO can be replaced by cerium doped indium oxide, which was shown in [38] to facilitate a broadband transparent contact with low electrical transport losses when sputter-deposited under the same hydrogen partial pressure as in case of the here applied ITO:H.

Future work will deal with a similar study on p-type contacts as well as the demonstration of the obtained findings on solar cell level.

References

[1] F. Feldmann, M. Bivour, C. Reichel, M. Hermle, and S. W. Glunz, "Passivated rear contacts for high-efficiency n-type Si solar cells providing high interface passivation quality and excellent transport characteristics," *Sol. Energy Mater. Sol. Cells*, vol. 120, pp. 270–274, 2014.

[2] J. Schmidt, R. Peibst, and R. Brendel, "Surface passivation of crystalline silicon solar cells: Present and future," *Sol. Energy Mater. Sol. Cells*, vol. 187, pp. 39–54, 2018.

[3] S. W. Glunz and F. Feldmann, "SiO_2 surface passivation layers—A key technology for silicon solar cells," *Sol. Energy Mater. Sol. Cells*, vol. 185, pp. 260–269, 2018.

[4] A. Richter *et al.*, "n-type Si solar cells with passivating electron contact: Identifying sources for efficiency limitations by wafer thickness and resistivity variation," *Sol. Energy Mater. Sol. Cells*, vol. 173, pp. 96–105, 2017.

[5] F. Feldmann, C. Reichel, R. Müller, and M. Hermle, "The application of poly-Si/SiOx contacts as passivated top/rear contacts in Si solar cells," *Sol. Energy Mater. Sol. Cells*, vol. 159, pp. 265–271, 2017.

[6] G. Nogay *et al.*, "Crystalline silicon solar cells with coannealed electron- and hole-selective SiC_x passivating contacts," *IEEE J. Photovolt.*, vol. 8, no. 6, pp. 1478–1485, Nov. 2018.

[7] R. Peibst *et al.*, "Industrial, screen-printed double-side contacted POLO cells," in *Proc. 33rd Eur. PV Sol. Energy Conf. Exhib.*, 2017, pp. 451–454.

[8] S. de Wolf, A. Descoeudres, Z. C. Holman, and C. Ballif, "High-efficiency silicon heterojunction solar cells: A review," *Green*, vol. 2, no. 1, pp. 7–24, 2012.

[9] J.-I. Polzin, F. Feldmann, B. Steinhauser, M. Hermle, and S. W. Glunz, "Study on the interfacial oxide in passivating contacts," in *Proc. AIP Conf.*, 2019, vol. 2147, Art. no. 40016.

[10] S. Lindekugel, H. Lautenschlager, T. Ruof, and S. Reber, "Plasma hydrogen passivation for crystalline silicon thin-films," in *Proc. 23rd Eur. Photovolt. Sol. Energy Conf. Exhib.*, 2008, pp. 2232–2235.

[11] M. K. Stodolny *et al.*, "n-type polysilicon passivating contact for industrial bifacial n-type solar cells," *Sol. Energy Mater. Sol. Cells*, vol. 158, pp. 24–28, 2016.

[12] G. Nogay *et al.*, "Interplay of annealing temperature and doping in hole selective rear contacts based on silicon-rich silicon-carbide thin films," *Sol. Energy Mater. Sol. Cells*, vol. 173, pp. 18–24, 2017.

[13] S. Mack *et al.*, "Metallisation of boron-doped polysilicon layers by screen printed silver pastes," *Phys. Status Solidi RRL*, vol. 11, no. 12, 2017, Art. no. 1700334.

[14] B. Nemeth *et al.*, "Polycrystalline silicon passivated tunneling contacts for high efficiency silicon solar cells," *J. Mater. Res.*, vol. 31, no. 6, pp. 671–681, 2016.

[15] M. Schnabel *et al.*, "Hydrogen passivation of poly-Si/SiOx contacts for Si solar cells using Al_2O_3 studied with deuterium," *Appl. Phys. Lett.*, vol. 112, no. 20, 2018, Art. no. 203901.

[16] A. Ingenito *et al.*, "Phosphorous-doped silicon carbide as front-side full-area passivating contact for double-side contacted c-Si solar cells," *IEEE J. Photovolt.*, vol. 9, no. 2, pp. 346–354, Mar. 2018.

[17] T. Koida, H. Fujiwara, and M. Kondo, "Hydrogen-doped In_2O_3 as high-mobility transparent conductive oxide," *Jpn. J. Appl. Phys.*, vol. 46, pp. 685–687, 2007.

[18] B. Macco *et al.*, "On the solid phase crystallization of In_2O_3: H transparent conductive oxide films prepared by atomic layer deposition," *J. Appl. Phys.*, vol. 120, no. 8, 2016, Art. no. 85314.

[19] M. Boccard, N. Rodkey, and Z. C. Holman, "High-mobility hydrogenated indium oxide without introducing water during sputtering," *Energy Procedia*, vol. 92, pp. 297–303, 2016.

[20] S. Husein *et al.*, "Carrier scattering mechanisms limiting mobility in hydrogen-doped indium oxide," *J. Appl. Phys.*, vol. 123, no. 24, 2018, Art. no. 245102.

[21] T. Koida, H. Fujiwara, and M. Kondo, "Hydrogen-doped In_2O_3 as high-mobility transparent conductive oxide," *Jpn J. Appl. Phys.*, vol. 46, pp. 685–687, 2007.

[22] B. Macco *et al.*, "Atomic layer deposition of high-mobility hydrogen-doped zinc oxide," *Sol. Energy Mater. Sol. Cells*, vol. 173, pp. 111–119, 2017.
[23] R. Chierchia, E. Salza, and A. Mittiga, "Effect of hydrogen gas dilution on sputtered Al:ZnO film," *Energy Procedia*, vol. 60, pp. 135–142, 2014.
[24] D. Gaspar *et al.*, "High mobility hydrogenated zinc oxide thin films," *Sol. Energy Mater. Sol. Cells*, vol. 163, pp. 255–262, 2017.
[25] S. Limpijumnong, P. Reunchan, A. Janotti, and C. G. van de Walle, "Hydrogen doping in indium oxide: An *ab initio* study," *Phys. Rev. B*, vol. 80, no. 19, 2009, Art. no. 193202.
[26] J. B. Varley, H. Peelaers, A. Janotti, and C. G. van de Walle, "Hydrogenated cation vacancies in semiconducting oxides," (in English), *J. Phys. Condens. Matter, Inst. Phys. J.*, vol. 23, no. 33, 2011, Art. no. 334212.
[27] A. S. Kale *et al.*, "Effect of crystallographic orientation and nanoscale surface morphology on poly-Si/SiOx contacts for silicon solar cells," (in English), *ACS Appl. Mater. Interfaces*, vol. 11, no. 45, pp. 42021–42031, 2019.
[28] S. de Wolf and M. Kondo, "Nature of doped a-Si:H/c-Si interface recombination," *J. Appl. Phys.*, vol. 105, 2009, Art. no. 103707.
[29] W. Kern and D. Puotinen, "Cleaning solutions based on hydrogen peroxide for use in silicon semiconductor technology," *RCA Rev.*, vol. 31, pp. 187–206, 1970.
[30] B. Steinhauser, J.-I. Polzin, F. Feldmann, M. Hermle, and S. W. Glunz, "Excellent surface passivation quality on crystalline silicon using industrial-scale direct-plasma topcon deposition technology," *Sol. RRL*, vol. 2, no. 7, 2018, Art. no. 1800068.
[31] B. W. H. van de Loo, B. Macco, J. Melskens, W. Beyer, and W. M. M. Kessels, "Silicon surface passivation by transparent conductive zinc oxide," *J. Appl. Phys.*, vol. 125, no. 10, 2019, Art. no. 105305.
[32] B. Macco *et al.*, "Influence of transparent conductive oxides on passivation of a-Si:H/c-Si heterojunctions as studied by atomic layer deposited Al-doped ZnO," *Semicond. Sci. Technol.*, vol. 29, no. 12, 2014, Art. no. 122001.
[33] Y. Wu *et al.*, "Enhanced doping efficiency of Al-doped ZnO by Atomic layer deposition using dimethylaluminum isopropoxide as an alternative aluminum precursor," *Chem. Mater.*, vol. 25, no. 22, pp. 4619–4622, 2013.
[34] R. Sinton, A. Cuevas, and M. Stuckings, "Quasi-steady-state photoconductance, a new method for solar cell material and device characterization," in *Proc. IEEE Photovolt. Specialists Conf.*, 1996, vol. 25, pp. 457–460.
[35] L. Tutsch *et al.*, "Integrating transparent conductive oxides to improve the infrared response of silicon solar cells with passivating rear contacts," in *Proc. AIP Conf.*, 2018, Art. no. 40023.
[36] T. F. Wietler *et al.*, "High temperature annealing of ZnO: Al on passivating POLO junctions: impact on transparency, conductivity, junction passivation, and interface stability," *IEEE J. Photovolt.*, vol. 9, no. 1, pp. 89–96, Jan. 2019.
[37] F. Feldmann *et al.*, "High and Low work function materials for passivated contacts," *Energy Procedia*, vol. 77, pp. 263–270, 2015.
[38] L. Tutsch *et al.*, "Implementing transparent conducting oxides by DC sputtering on ultrathin SiOx/poly-Si passivating contacts," *Sol. Energy Mater. Sol. Cells*, vol. 200, 2019, Art. no. 109960.
[39] F. Lebreton, S. N. Abolmasov, F. Silva, and P. Roca i Cabarrocas, "In situ photoluminescence study of plasma-induced damage at the a -Si: H/c-Si interface," *Appl. Phys. Lett.*, vol. 108, no. 5, 2016, Art. no. 51603.
[40] M. Lozac'h, S. Nunomura, H. Umishio, T. Matsui, and K. Matsubara, "Hydrogen passivation effect on p-type poly-Si/SiOx stack for crystalline silicon solar cells," in *Proc. AIP Conf.*, 2019, vol. 2147, Art. no. 40010.
[41] N. Juneja *et al.*, "Effect of hydrogen addition on bulk properties of sputtered indium tin oxide thin films," in *Proc. AIP Conf.*, 2019, vol. 2147, Art. no. 40008.